Photodiagnosis and Photodynamic Therapy 21 (2018) 98–107

Contents lists available at ScienceDirect

Photodiagnosis and Photodynamic Therapy

journal homepage: www.elsevier.com/locate/pdpdt

# Photodynamic therapy in fibrosarcoma BALB/c animal model: Observation of the rebound effect

Etcheverry María Eugenia[a], Pasquale Miguel Ángel[a], Gutiérrez Anabella[b], Bibé Solange[b], Ponzinibbio Carlos[b], Poteca Horacio[c], Garavaglia Mario[d,e,*]

[a] Instituto de Investigaciones Fisicoquímicas Teóricas y Aplicadas (INIFTA) (CCT CONICET La Plata, UNLP y CIC), Argentina
[b] Cátedra de Patología B, Facultad de Ciencias Médicas, Universidad Nacional de La Plata, CP 1900, Argentina
[c] Centro Médico Láser, La Plata, Buenos Aires, Argentina
[d] Centro de Investigaciones Ópticas (CIOp) (CCT CONICET La Plata, UNLP y CIC), Argentina
[e] Departamento de Física, Facultad de Ciencias Exactas, UNLP, Argentina

ARTICLE INFO

*Keywords:*
Photodynamic therapy
Fibrosarcoma
Fluorescence spectra
Photosensitizer accumulation

ABSTRACT

In vivo spectrofluorometric analysis during photodynamic therapy (PDT) is a fundamental tool to obtain information about drug bleaching kinetics. Using a portable spectrofluorometer with an excitation source emitting at 400 nm wavelength and a spectral analyzer ranging from 500 nm to 800 nm, the evolution of the meta-tetra (hydroxyphenyl) chlorin (m-THPC) photosensitizer fluorescence spectrum at the tumoral tissue of BALB/c murines with fibrosarcoma located at their flank was followed up. Ex vivo fluorescence measurements of the tumor and skin were also performed with the aim of better characterizing the in vivo signal at different parts of the tumor. PDT was performed employing a LED 637 nm light source. Fluorescence at different parts of the tumor and at the tail and armpit of mice was measured immediately after injection and followed daily. The average fluorescence intensity in the tumor reached a maximum after 24–72 h. Subsequently, illuminations 24, 48, 72 and 96 h post-injection were performed, and the fluorescence was measured immediately before and after each illumination. Eventually, 24 h post-illumination, the fluorescence at certain parts of the tumor increased in comparison with that measured immediately after illumination. This effect, named "rebound effect", was due to the new local accumulation of the drug, and was used to perform a second illumination on some mice to increase the amount of photodynamic reaction and significantly improve the PDT outcome. These results are encouraging to optimize PDT in the proposed animal model, thinking about the possible translation to humans.

## 1. Introduction

Photodynamic therapy (PDT) centers on the photochemical interaction of three principal components: oxygen, photosensitizer, and light. This treatment modality uses light of an appropriate wavelength in the presence of oxygen to activate a photosensitizing drug, which then causes tumoral cell death. Singlet oxygen ($^1O_2$) and other reactive oxygen species (ROS) are generally believed to be the major cytotoxic agents during PDT [1–5].

The current use of PDT in oncology dates back to the early 1970's, when T. J. Dougherty began his investigations into the mechanisms and clinical uses of hematoporphyrin derivatives (HpD) [6–8]. Although PDT can mediate many signaling events in cells, its main purpose is generally to kill cells. Recent research has elucidated many pathways whereby mammalian cells can die, and some of the ways that PDT can initiate these processes [9]. The concentration, physicochemical properties and subcellular location of the photosensitizer (PS), the concentration of oxygen, the appropriate wavelength and intensity of the light, the specific cell type and tissue environmental properties may all influence the mode and extent of cell death [10,11]. It has been suggested that apoptosis and necrosis share common initiation pathways and that the final outcome is determined by the presence of an active caspase [10]. This implies that apoptosis inhibition reorients cells to necrosis, i.e., those cells sufficiently damaged by PDT appear to be killed, regardless of the mechanism involved. It is also worth noting that PDT induces membrane degradation. Thus, substances are released within vasculature and interstitium. Some of these substances are directly toxic, while others may activate immune responses [12] and impact vascular responses with platelet activation and alteration in vascular permeability ranging from constriction to leakage [13,14]. Furthermore, PDT causes acute inflammation, invasion and infiltration of the tumor by leukocytes and might enhance the production of tumor-

* Corresponding author at: Centro de Investigaciones Ópticas (CIOp) (CCT CONICET La Plata, UNLP y CIC), Argentina.
*E-mail address:* garavagliam@ciop.unlp.edu.ar (G. Mario).

https://doi.org/10.1016/j.pdpdt.2017.11.006
Received 6 June 2017; Received in revised form 11 October 2017; Accepted 15 November 2017
Available online 16 November 2017
1572-1000/ 

derived antigens to T cells [15–17].

On the other hand, the application of HpD fluorescence detection of tumoral tissue for clinical use started with R.L. Lipson and colleagues [18]. In porphyrins, the absorption of light in the 400 nm range characterized by the Soret band is employed for diagnosis, as in this case there is a large Stokes shift between the excitation and emission bands. The fluorescent signature can also be used as an optical biopsy to determine benign versus malignant disease without the need for histological evaluation [19].

The interaction of light with tissue results in attenuation of the incident light energy due to reflectance, absorption, scattering, and refraction. Refraction and reflection are reduced with perpendicular light application because of the Fresnel law, whereas absorption can be minimized by the choice of a photosensitizer that absorbs in the far-red region of the electromagnetic spectrum. At these wavelengths, the tissue optical window is optimal for PDT application [2]. The clinical application of PDT has improved considerably due to the development of new more efficient and selective photosensitizers, new devices, and the design of more appropriate protocols to modulate PDT response [20,21].

Fluorescence measurements have been utilized to determine meta-tetra(hydroxyphenyl) chlorine (m-THPC) and a water-soluble derivative biodistribution in a human colorectal adenocarcinoma implanted in Swiss nude mice [22,23]. Although PS fluorescence in the tumor after 72 h was greater than that 24 h post-administration, better results have been reported for PDT performed 24 h post m-THPC administration, setting a limit for this technique [22]. It has been claimed that fluorescence measurements before PDT could improve the correlation between the administered light dose and the treatment outcome of esophagus carcinomas [24,25]. Other publications reported the importance of in vivo measurement of the reduction of PS concentration during treatment [26]. Of particular interest is the change in fluorescence during therapy, which may be an excellent dosimetric guide to modification of illumination [26–37]. Provided the difference in fluorescence prior, during, and after the photodynamic treatment is measured accurately, it could be used to evaluate the potential success or failure of the proposed curative or palliative protocol. Tissue optical properties affect both the light dose participating at the photochemical reaction and the fluorescence signal detection. For instance, 5-aminolevulinic acid (PpIX) fluorescence measurements have been corrected by reflectance during PDT in sensitized normal rat skin [38]. Furthermore, it has been possible to monitor interstitial m-THPC-PDT simultaneously measuring light fluence, fluorescence, blood oxygen saturation, and blood volume without interrupting the therapeutic illumination [39]. In this case, a complex relationship between the fluence rate and m-THPC fluorescence photobleaching has been obtained.

Many techniques to detect fluorescence of PpIX in relation to PDT in neoplastic skin have been employed according to the properties of the target tissue [40]. Provided fluorescence measurement limitations are known, it is an accessible parameter to be evaluated clinically in a PDT treatment [41].

In this paper, results from in vivo fluorescence measurements before and at different times during PDT application in a fibrosarcoma (TMC) animal model employing a 637 nm LED lamp are presented. Average data are used to infer the amount of the drug photochemical reaction at different sites, and to improve the illumination protocol. Furthermore, ex vivo fluorescence measurements are utilized to discriminate contributions to in vivo fluorescence from the different components of the tumor model. The results indicate that drug concentration in the tumor is maximal at 48 h, and after illumination, the decrease in fluorescence depends on the location in the tumor; while some parts exhibit pronounced signal depletion, others remain roughly constant. Fluorescence measurement 24 h post-illumination indicates an increase in the concentration of photosensitizer relative to that obtained immediately after the illumination, “rebound effect”, particularly in the apical region of the tumor. Thus, a second illumination is performed to induce more reaction and tumor cell killing. These results are useful to design improved protocols for clinical PDT in humans.

## 2. Materials and methods

### 2.1. Induced tumors in BALB/c mice

BALB/c mice fed with alfalfa-free sterilized pellets were utilized. Tumors in BALB/c mouse flanks were induced with methylcholanthrene [42,43] and were subcultivated by subcutaneously inoculating cells from the tumor in the right flanks of healthy mice. After about two weeks, tumors of size between 0.4 and 0.8 cm in diameter were obtained. Mice with tumors that are detected by touch and with similar geometrical characteristics were selected for this work.

Eventually, tumors were excised from mice and immediately fixed by immersion in 4% neutral buffered formalin solution. Fixed tumors were cut and placed in embedding cassettes, and processed according to the standard protocol. Briefly, samples were dehydrated by immersion in ethanol solutions of increasing concentration (70, 80, 95 and 100% ethanol), xylene, embedded in paraffin, and cut into 5 μm sections. Dried sections were deparaffinized using xylene, 96% ethanol and 70% ethanol, rehydrated and stained with hematoxylin and eosin. The images were taken with a BX51 Olympus microscope (Olympus Co., Japan).

### 2.2. Drug administration and fluorescence measurement

The photosensitizer meta-tetrahydroxyphenyl chlorin (m-THPC) (Foscan$^{R}$, Biolitec Pharma Ltd. United Drug House, Magna Drive Dublin 24, Ireland), diluted in a mixture of ethanol/propylene glycol (2:1 molar ratio), was administrated to mice by injection at the medial portion of the tail with a dose in the range 0.75–1.60 mg/kg of the animals. The animals were held in a dark cage, according to the recommendations of the protocol to avoid unwanted effects of the therapy, particularly in mouse eyes.

The fluorescence signal related to the photosensitizer concentration at different regions of the tumor and different times (Fig. 1a and b) was determined by a point fluorescence detection technique. In fact, these measurements also include the contribution of the skin, but on average reflect the evolution of m-THCP in the tumor (Section 3.5). The fluorescence spectra at the mice were obtained by exciting at 400 nm using a fluorometer (JETI Technische Instrumente GmbH) provided with an appropriate dual-pass fiber optics 0.20 mm in diameter, which allows simultaneous local excitations and emission measurements of the studied area (Figs. 1 a and Fig. 2). The fluorescence spectrum in the 500–800 nm range was recorded, and the fluorescence intensity associated with m-THPC emission was obtained from the maximum at 652 nm prior to subtraction of the baseline due to the autofluorescence of each sample. Proximal and distal portions of the tail, the left armpit, four apical sites (1, 2, 3, 4) and lateral regions (cranial, dorsal, ventral and caudal) of the tumor were measured (Figs. 1a and b). Measurements at different times were performed guided by marks done on the surface of the tumor to minimize errors due to location of the fiber-optic tip at each site (Fig. 1a).

In another set of experiments, we proceeded according to the schedule: (i) mice previously injected with 0.75 mg/kg of photosensitizer were sacrificed after 48–72 h, and the skin-covered tumor was excised. Then, fluorescence signals at different sites of the skin-covered tumor were obtained (Fig. 1b). Subsequently, the skin was separated from the tumor, and fluorescence measurements at the same locations were obtained from the tumor and the skin separately, in order to discriminate the contribution of each other to the total fluorescence. (ii) Mice previously injected with 0.75 mg/kg of photosensitizer were illuminated 48 h after injection and sacrificed, and fluorescence measurements were performed immediately as indicated

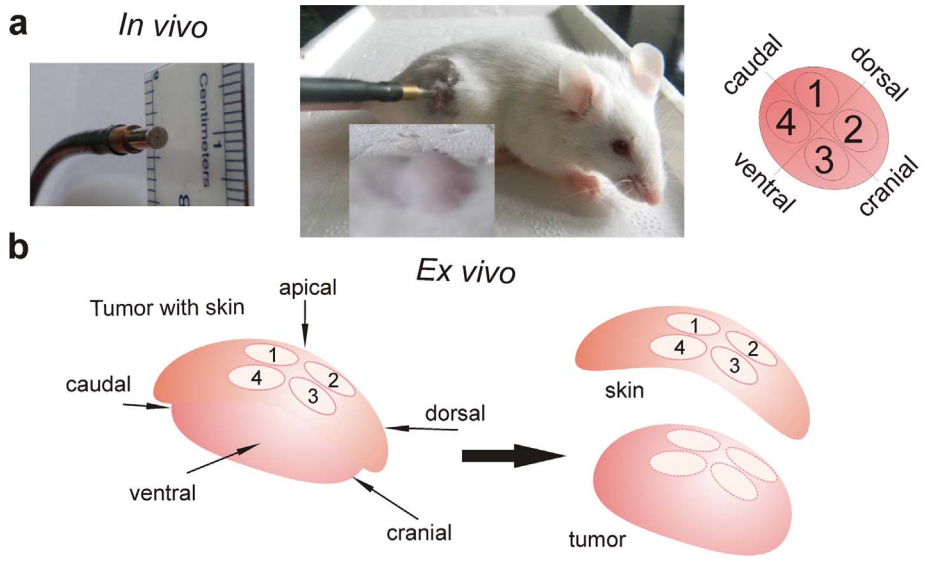


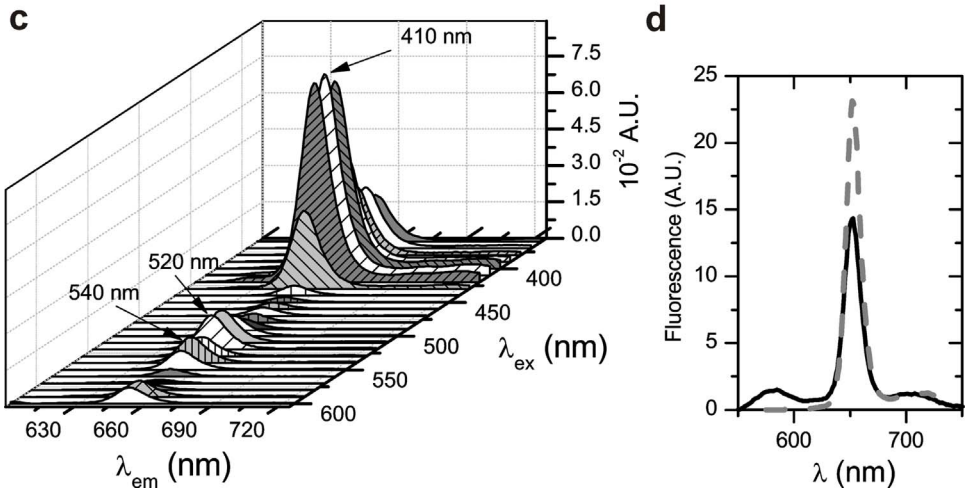


**Fig. 1.** One-point fluorescence measurement at the mouse tumor. (a) Images of the fiber optics utilized in the measurements and its location in the tumor. A typical tumor image is also depicted. Scheme of the different tumor sites where fluorescence was measured: apical sites shown as 1, 2, 3, and 4; lateral sites named cranial, dorsal, ventral and caudal sites. (b) Scheme of the procedure followed to perform ex situ fluorescence measurements at the skin-covered tumor and the skin and tumor separately. (c) Fluorescence excitation/emission spectra of m-THCP 1 mM in methanol. Arrows indicate the wavelengths of m-THPC absorption maximum. (d) Typical fluorescence spectrum measured at the tumor of a mouse injected with m-THPC at a dose of 1.4 mg/kg (solid line). The fluorescence spectrum of m-THPC in methanol is depicted in dashed line.

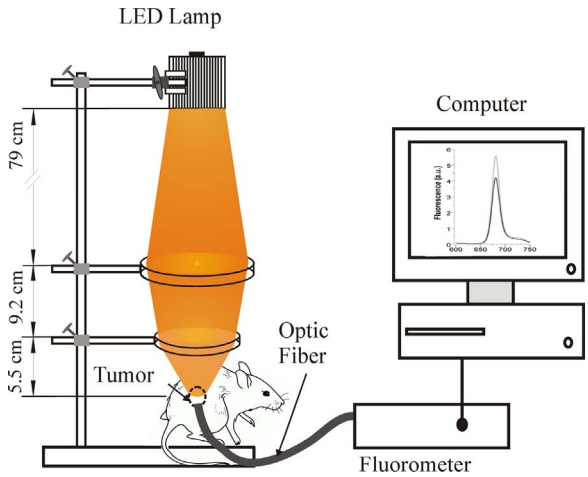


**Fig. 2.** Scheme of the experimental arrangement to measure fluorescence and perform PDT treatment.

in (i).

The m-THPC excitation/emission spectra from the tumor and a solution in methanol are depicted in Fig. 1c and d. The largest fluorescence intensity in both cases is obtained by illuminating with a wavelength close to 400 nm, i.e., the Soret band. Then, although tissue absorption is larger at 400 nm, i.e., of the order of 90%, the transmitted light is enough to excite the m-THCP, which subsequently fluoresces at 652 nm, 50% being transmitted through the tissue optical window [44].

Besides, according to the Jasblonsky diagrams [45], the highest fluorescence intensities at 652 nm are coincident with the m-THPC absorption peak used in these experiments for PDT applications. However, at the excitation wavelength (400 nm) the absorption is much larger than at 652 nm and the m-THCP fluorescence quantum yield is high, 0.22 [46]. The fluorescence signal measured five times successively at the same site of the tissue remained constant on average.

Light of wavelength between 400 and 650 nm transmitted through the skin and tumor slices with controlled thickness was measured employing a spectrometer (Ocean Optic USB 2000 + ) provided with a fiber optics and appropriate 1W output LED sources and lenses located conveniently on an optical bench. Tumor slices were placed between two planar quartz crystals separated by Teflon spacers (Good Fellow, England) of known thickness and located on the optical bench with a sample holder to ensure perpendicular incidence of light.

### 2.3. Treatment

Mice were illuminated with a light dose of 20 J/cm$^2$ following the recommendation of Foscan$^R$ leaflet. An experimental arrangement consisting of a LED lamp and appropriate condensing lens to illuminate the desired area rendering a luminous flux of 130 lm [47] (Fig. 2) was employed. The fluence rate was 54 mW/cm$^2$ and the illuminance at the

distance of work was 0.113 mW/cm$^2$, and the amount of light delivered by the LED lamp was from 34 lms/cm$^2$ to 68 lms/cm$^2$ at 0.79 m for 5–10 min of illumination respectively [47].

The animals were placed in such a way that the illuminated surface strictly corresponded to the tumor region. In some cases, fluorescence measurements were used to better delimitate the extension of the tumor, as areas that appeared as normal by eye observation retained abnormal photosensitizer concentration.

To protect the animals from the effect of light illumination on other parts of their bodies, they were covered with double black cloth so that only the tumor area was exposed. The lighting time was controlled by a timer connected directly to the LED lamp switch.

### 2.4. Indexes to estimate the amount of photodynamic reaction

Following indications in the literature [48,49], three different indexes defined below were used to describe the decrease in the fluorescence signal after the application of light to the murine tumor according to the designed protocol for treatment.

I1 = 100 x (fluorescence before the first illumination – fluorescence after the first illumination)/fluorescence before the first illumination

I2 = 100 x (fluorescence before the second illumination – fluorescence after the second illumination)/fluorescence before the second illumination

I3 = 100 x (fluorescence before the second illumination – fluorescence after the second illumination)/fluorescence after the first illumination.

The comparison between I3 and I2 is an indication of the magnitude of the “rebound effect”, as I3 includes the fluorescence immediately after the first illumination as quotient and I2 the fluorescence 24 h after the first illumination. Then, the difference is related to the accumulation of new photosensitizer in the treated region.

## 3. Results and discussion

### 3.1. Fluorescence measurements along time, Determination of the maximum drug concentration

As photosensitizer accumulation in the animal model varies with time, after injection with an m-THPC dose of 0.75 mg/kg, the evolution of the concentration of m-THPC was followed up by measuring the corrected fluorescence signal at 652 nm, where a characteristic peak for this photosensitizer was observed.

The evolution of the fluorescence intensity at 652 nm, taken from different sites in the animal model, is shown in Figs. 3 and 4. In Fig. 3, fluorescence data were obtained by averaging over different sites of the skin-covered tumor and over different tumors. The photosensitizer maximum concentration at the tumor tissue was observed for a time interval between 24 h (≈ 38 AU.) and 96 h (≈ 28 AU.) after drug administration (Fig. 3). Average fluorescence measurements started to diminish after about 100 h, and for 256 h the signal decreased to about 10 AU. Then, the photosensitizer concentration becomes low to perform the therapeutic illumination.

In another set of experiments, the average fluorescence intensity along time was read from the armpit, apical, cranial, ventral, dorsal and caudal sites of the skin-covered tumor, and the results are depicted in Fig. 4. The average was performed considering seven measurements per site, and the standard error is included.

From measurements of fluorescence at the tumor sites, the maximum intensity was observed in the 24–48 h range, but depended on the site of the tumor. Maximum values of 46, 58, 30, 45 and 45 AU. were obtained from the cranial, caudal, apical, dorsal and ventral sites, respectively (Fig. 4). Differences between fluorescence intensity values measured at a constant time and at different sites of the tumor reflect its heterogeneity. Images of different sections of tumors similar to those used for PDT revealed noticeable cell morphological differences

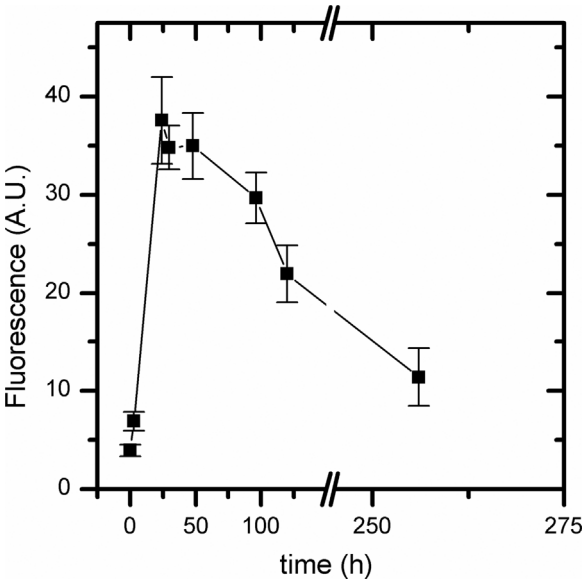


**Fig. 3.** Average fluorescence intensity of the tumor measured from the m-THPC spectrum maximum at 652 nm. Measurements were performed at different times (indicated in the figure) after the photosensitizer injection at a dose of 0.75 mg/kg. Data were obtained by averaging measurements at different sites of the tumor. The standard errors are included, and four animals were considered.

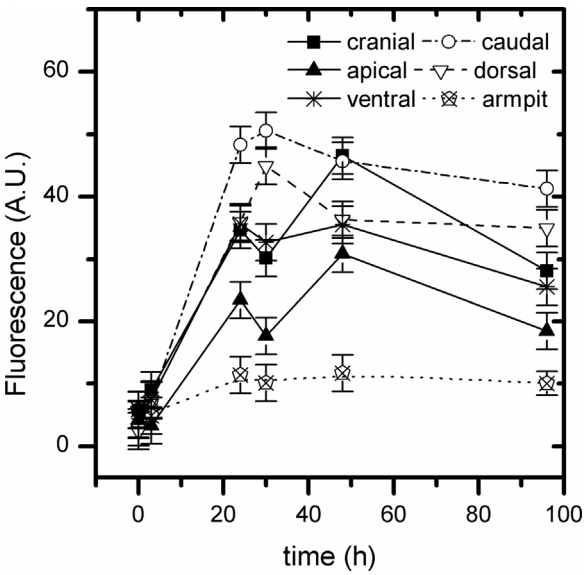


**Fig. 4.** Typical fluorescence measurements at different sites of the tumor along time, as indicated in the figure. Animals were injected with 0.75 mg/kg m-THPC. The errors were calculated from four measurements for each different site of the tumor.

depending on the region of the tumor. For the largest tumors, necrotic zones can also be observed (this is further described in Section 3.4).

After 24–96 h of photosensitizer injection, the fluorescence signal from any site of the tumor was larger than that obtained from the armpit (Fig. 4). Thus, the preferential accumulation of the drug in the neoplastic tissue was observed. Fluorescence from the armpit is produced mainly by the skin, while measurements on the tumor include the contribution of the skin. While fluorescence from the armpit increases up to 48 h and afterwards remains constant, the average fluorescence signal from the tumor starts to decrease at 48 h. This may reflect the difference in the photosensitizer uptake by the skin and the tumor.

As expected, the maximum fluorescence signal was observed at the proximal or eventually at the distal region of the tail, near the drug

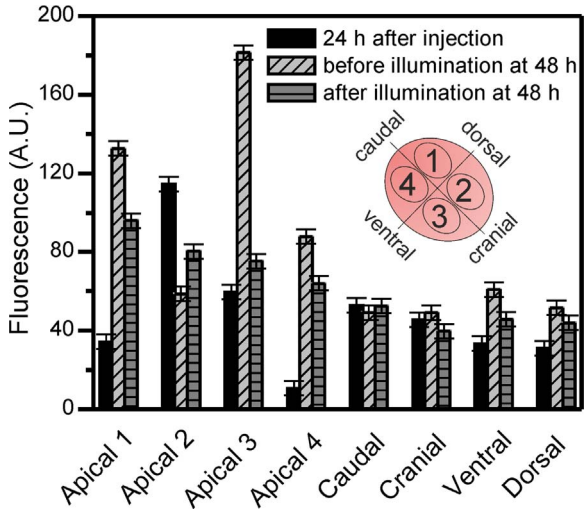


**Fig. 5.** Typical average fluorescence intensity measurements at apical, caudal, cranial, ventral and dorsal sites 24 h after injection, 48 h before and after illumination. At the beginning, the tumoral area was close to 4 mm x 4 mm in all the cases. Mice were injected with m-THPC 0.75 mg/kg and after 48 h, they were illuminated for 13 min.

injection site. This indicates that some extravasation occurred at the injection site in spite of the fact that the drug was well distributed by the blood flow.

### *3.2. Fluorescence measurements at different tumor sites before and after illumination. PDT treatment with a single illumination*

Average fluorescence measurements at different sites of the tumor, before and immediately after illumination at 48 h post-injection are shown in Fig. 5. Apical and lateral tumor regions are considered. In the apical region of the tumor, measurements are performed at four sites (1, 2, 3 and 4) and in the lateral region at cranial, caudal, dorsal and ventral sites as indicated in (Fig. 1). In most of the cases, the fluorescence increased after injection of m-THPC at a dose of 0.75 mg/kg, and before illumination it was significantly larger than immediately after illumination. This indicates that the reaction of the photosensitizer occurs at the applied light dose.

The largest changes in fluorescence, before and immediately after illumination, were measured for apical sites; a change close to 100 AU. was observed for the “apical site 3” (Fig. 5). For “apical sites 1 and 4” a similar relative decrease in the fluorescence, about 1.4, was observed immediately after illumination. For “apical site 2” no decrease after illumination was observed.

The decrease in the fluorescence after the first illumination, measured at the lateral sites of the tumor, was significantly smaller than in the apical regions. This is in part consistent with the geometry of the tumor that restricts the amount of light that reaches the lateral regions. It is worth noting that the heterogeneity of tumors would affect their response towards illumination, and each site would exhibit a particular behavior [50]. Fluorescence measurements are largely influenced by the presence of blood in the examined tissue due to the low transmittance of the excitation light at 400 nm, as will be discussed in Section 3.5. Experimental tumors contain a significant fraction of microregions that are chronically or transiently hypoxic. There is increasing experimental evidence showing that hypoxia (and subsequent reoxygenation) may have a profound impact on malignant progression and on responsiveness to therapy [51,52]. As will be described in the next section, for apical sites, fluorescence measurements 24 h after illumination tend to exhibit a higher value than immediately after illumination, but this is not the case for all the measured sites.

The importance of the tissue geometry and the incidence angle of light in determining the optimal dosimetry for an effective PDT treatment have been reported [53]. In this work, it has been indicated that the internal light distribution should be considered in order to avoid misleading conclusions. Furthermore, it is important to place the light source perpendicular to the tumor, in order to minimize errors that alter the photon fluence inside the tumor, but if the incidence angle is smaller than 15° in the PDT treatment, it is not necessary to adjust the incidence angle [53].

A plausible correlation between fluorescence and the m-THPC concentration should depend on the tissue optical properties. In our case, provided the optical properties remain constant in time at each site, the fluorescence would be indicative of the photosensitizer concentration even when the tumor is highly heterogeneous. For the time range of our fluorescence measurements, despite the high reactivity of singlet oxygen, the tissue structure remained unchanged according to histological data, and a feasible comparison between measurements before and after illumination is expected to be appropriate. Thus, it is important to control the location of the fiber optics at each site along the whole observation at the different stages of the experiment.

### *3.3. Fluorescence measurements along time. Double illumination PDT treatment*

As discussed in the previous section, for mice injected with 0.75 mg/kg, in most parts of the apical region the fluorescence immediately after illumination showed a significant decrease due to the reaction of the photosensitive drug with light coming from the LED lamp. But interestingly, 24 h after the first illumination, the intensity of the fluorescence signal measured at the same sites showed that it eventually remained constant, decreased or increased in relation to the one obtained immediately after illumination (Figs. 6 and 7). The increase of the fluorescence signal, which we call “rebound effect”, would indicate the presence of fresh photosensitizer at certain sites that can be employed to generate more neoplastic tissue destruction by delivering light through a new illumination. The effectiveness of the photodynamic reaction is shown by the decrease of the fluorescence signal immediately after the second illumination. A similar observation has been recently reported. In fact, the replenishment of photofrin after 5 h of illumination was reported for a radiation-induced fibrosarcoma in C3H mice [29], although no further illumination was performed.

Fluorescence data were obtained after correction due to tissue autofluorescence; as shown in Fig. 6b, all curves are referred to the same baseline. It is worth noting that the fluorescence signal evolution depended on the site of measurement at the tumor due to its heterogeneity, and it should change from one animal to another. Nevertheless, average fluorescence data from the apical tumor sites of five mice (Fig. 7a) exhibited a significant increase in the fluorescence 24 h after the first illumination and a subsequent decrease after the second illumination.

Furthermore, the indexes I1, I2 and I3 (see the Materials and Methods Section) are useful to quantify the improvement in the amount of reaction caused by a single or double illumination. The indexes compare the fluorescence before and after illumination, in relation to the fluorescence before the first illumination (I1), the fluorescence before the second illumination (I2), and that after the first illumination (I3). The latter index would be indicative of the amount of photochemical reaction and would take account of the net balance of photosensitizer, coming from non-illuminated zones and disappearing probably due to metabolism, in a range of time comprised between the first and the second illumination. For the apical region of the tumor, average data from different sites show that in most of the cases I1 is larger than I2 and I3 (Fig. 7), contrary to the site “apical 2” where $I3 > I2 > I1$ can be inferred (Fig. 6). These data would indicate that the “rebound effect” can be useful to increase the amount of reaction at least at certain sites of the tumor.

Mice injected with a dose of 1.40 mg/kg of m-THPC showed an increased average value of the fluorescence signal in the apical region

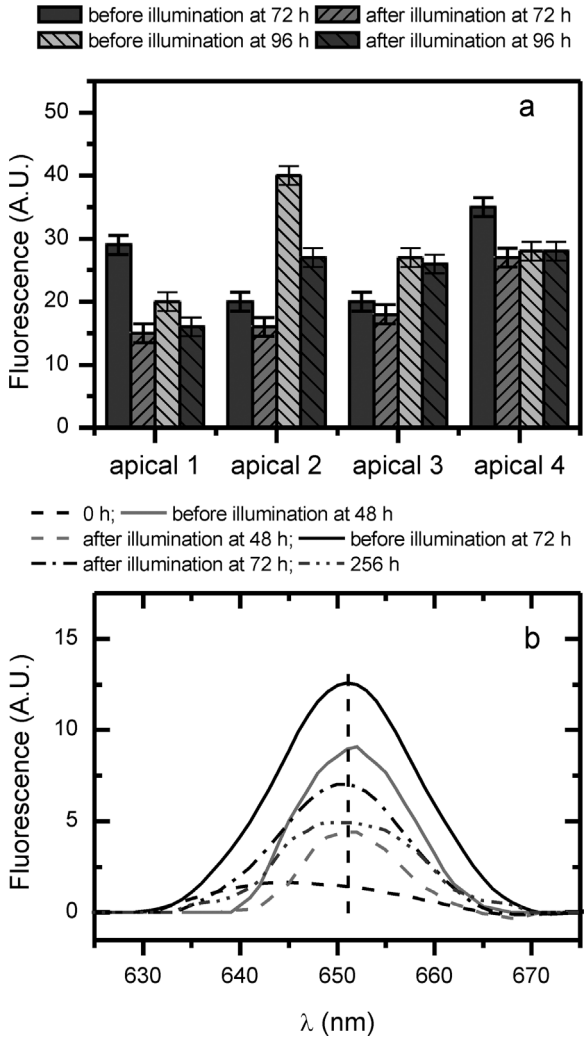


**Fig. 6.** Fluorescence signal measured at the apical region of a tumor. The mouse was injected with a dose of 0.75 mg/kg. The first illumination was performed at 72 h and the second, 96 h after drug injection (a). The first illumination was performed at 48 h and the second, 72 h after drug injection (b).

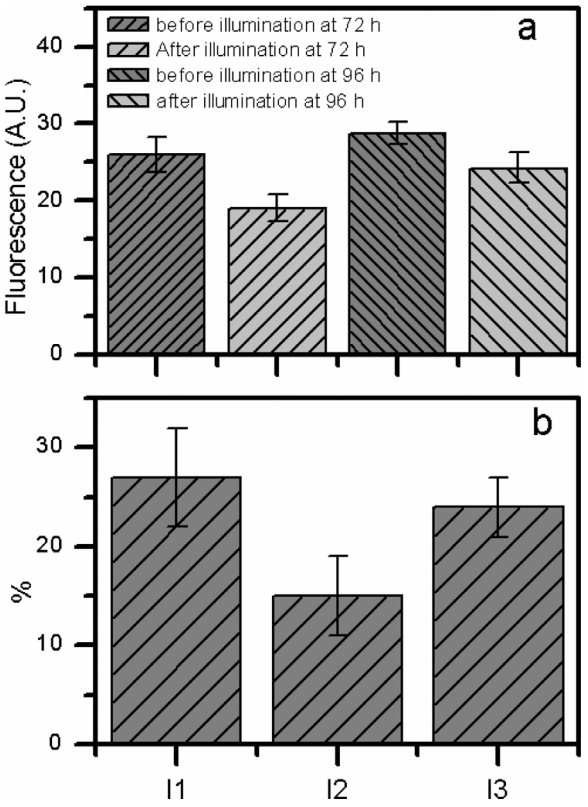


**Fig. 7.** Average fluorescence measurements before and after the first and second illumination at times indicated in the figure (a). Average indexes I1, I2 and I3 calculated for the four sites of the apical region of the tumor (b). The photosensitizer was injected at a dose of 0.75 mg/kg. The first illumination was performed at 72 h and the second, 96 h after drug injection.

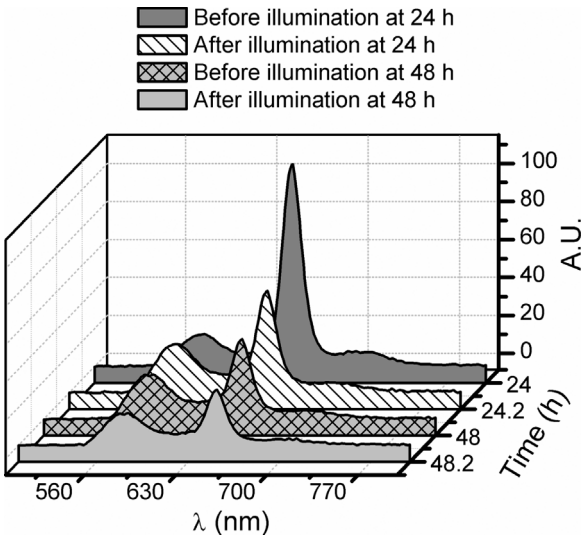


**Fig. 8.** Average fluorescence spectra at 600–700 nm from the apical zone of the tumor of a mouse injected with the photosensitizer at a dose of 1.40 mg/kg. The first illumination was performed at 24 h and the second, 48 h after drug incorporation.

24 h after injection in comparison with the mice injected with 0.75 mg/kg of m-THPC (Figs. 7 and 8). Furthermore, a clear decrease in the signal was observed after the first illumination. Subsequently, 24 h post-illumination, the fluorescence signal at 652 nm remained almost at the same level, close to a value of 50 AU., which decreased to 10 AU. after a second illumination with the same light dose indicated above. It can be hypothesized that the photosensitizer metabolism would produce a more significant decrease in the fluorescence, which was not observed in our experiments. Thus, new fresh photosensitizer was flown into the tumor at zones with healthy vasculature. In this case, a double illumination would improve the PDT outcome.

The ratio between the fluorescence measured at 652 nm, before and after the second illumination, was significantly larger for the experiment with the mice injected with 0.75 mg/kg (Fig. 6) than for the mice injected with 1.4 mg/kg (Fig. 8), i.e., 2.33 for the lower concentration and 1.65 for the larger concentration. This can be explained by the requirement of more illumination and oxygen in the case of a larger drug concentration. Thus, a larger drug concentration does not imply a better PDT effect [54]. So, the photodynamic therapy must involve the appropriate amount of light with a specific wavelength and oxygen to assure the PDT reaction. In this regard, it has been reported that fluorescence measurements are limited to predict the PDT outcome, as a higher fluorescence obtained at 72 h post injection in comparison with that obtained at 48 h post-injection has no correlation with the better results achieved when illuminating at 48 h post-injection [22].

### 3.4. Tumor histology

Tumor histology is useful to interpret fluorescence data. In this subsection a brief histological description of the tumor is given, and in the next subsection the optical properties of the skin and tumor are

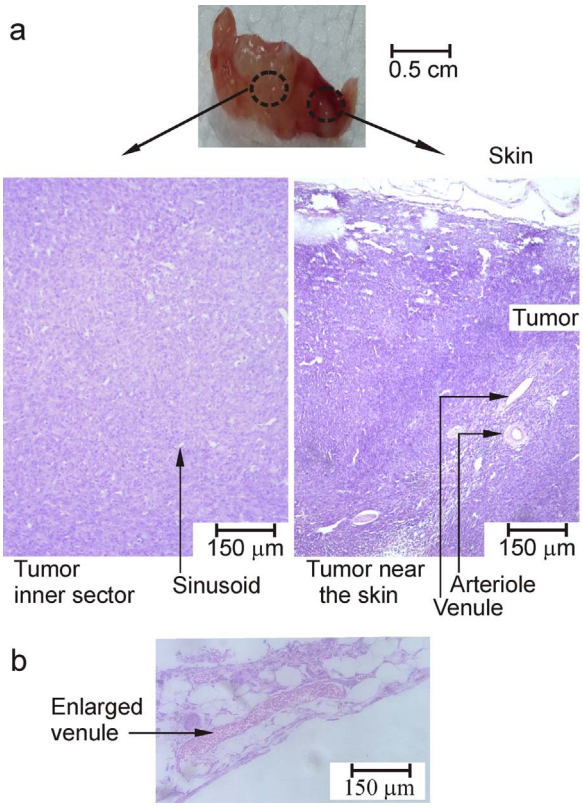


**Fig. 9.** Image of a typical excised tumor (a). Partial picture of a hematoxylin-eosin stained tumor slice (b). At the region of attachment to the skin, the tumor exhibits a large number of enlarged vessels. At the central region, vessels are smaller and rather homogeneously distributed. An enlarged venule in the skin over the tumor is also depicted in the figure.

discussed. A typical tumor, obtained after two weeks of tumor cell inoculation in the right flank of a mouse, was excised and carefully trimmed and placed in the paraffin embedding cassettes, maintaining its actual orientation in the mouse flank. This type of tumor consists of a malignant connective (soft) tissue originated in fibroblasts. The tumor appears as a compact mass of anaplastic fibroblasts, some of them with a spindled form and with architectural disarray. The tumor is usually fed by vasculature from the dermis as larger vessels are seen in proximity of the skin, while the tumor central section shows smaller sinusoids homogenously distributed all around the tumoral tissue. In this case, the tumor was attached by one end to the dermis, where a rather large vessel can be distinguished (Fig. 9a). Concomitantly, a larger number of arterioles and venules were observed in the region of tumor-skin attachment (Fig. 9b). Furthermore, a portion of the skin above the tumor exhibited venules with augmented size, in which fixed erythrocytes can be distinguished. On the other hand, in most parts of the tumor, a rather homogeneous vessel distribution was observed (Fig. 9c), at least at the mm scale, the size of the fiber optics used in the fluorescent measurements.

### 3.5. Ex vivo and fluorescent measurements

The intensity of light passing through the mouse skin that covers the tumor was measured employing a fiber optic spectrometer and LED sources of 400 and 652 nm. Samples were placed in a sample holder with plane quartz windows. For 652 nm the measured intensity was 6–10 times higher than for 400 nm (Fig. 10a). The smaller values were obtained from regions with a relatively high concentration of blood vessels. The reported BALB/c mouse skin transmittance was close to 50% at 652 nm and about 5% at 400 nm [44,55].

On the other hand, the average intensity of light of 400 nm and 652 nm that passes through a portion of tumor of different thickness ($h$)

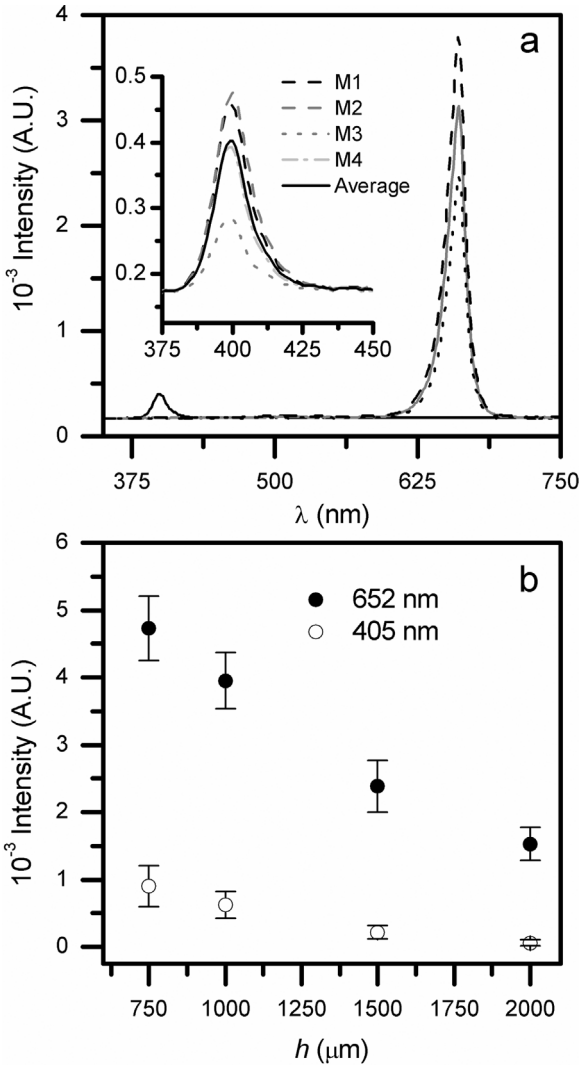


**Fig. 10.** Intensity of light transmitted by the skin covering the tumor at 400 and 652 nm (a). Four different spectra obtained at different sites of the skin are included (inset). The smallest signal is obtained from regions with a large density of blood vessels. (b) Dependence of the transmitted light intensity on the tumor thickness.

ranging from 750 to 2000 μm is plotted in Fig. 10 b. The intensity of the signal decays monotonously with $h$ for both wavelengths. For 652 nm and $h = 750$ μm, the intensity approaches 4700 AU. and for $h = 2000$ μm, it is close to 1650 AU. For 400 nm the intensity reaches a value close to 920 AU. for $h = 750$ μm and diminishes to 100 AU. for $h = 2000$ μm. These data would indicate that the fluorescence detected in vivo would reflect the presence of m-THPC in the skin and the tumor.

Ex situ fluorescence measurements were performed to discriminate the contribution of the skin and the tumor itself to the total fluorescence signal (Fig. 11). Six mice were injected with m-THPC at a dose of 0.75 mg/kg and after 48 h three mice were sacrificed before illumination and other three immediately after illumination. Fluorescence was measured within four hours after mice sacrifice at (i) the excised skin-covered tumor, (ii) the tumor without the skin, and (iii) the skin. In all the cases, measurements were carried out placing the fiber optics at four different apical sites, as indicated in Fig. 1. In most of the cases, fluorescence measurements were on average larger before illumination than immediately after illumination. This indicates that the reaction of the photosensitizer occurs at the applied light dose as in the case of in vivo measurements. The largest signals were obtained from sites at skin-covered tumor and the tumor without skin. In contrast, fluorescence from sites at the skin was significantly smaller. Average

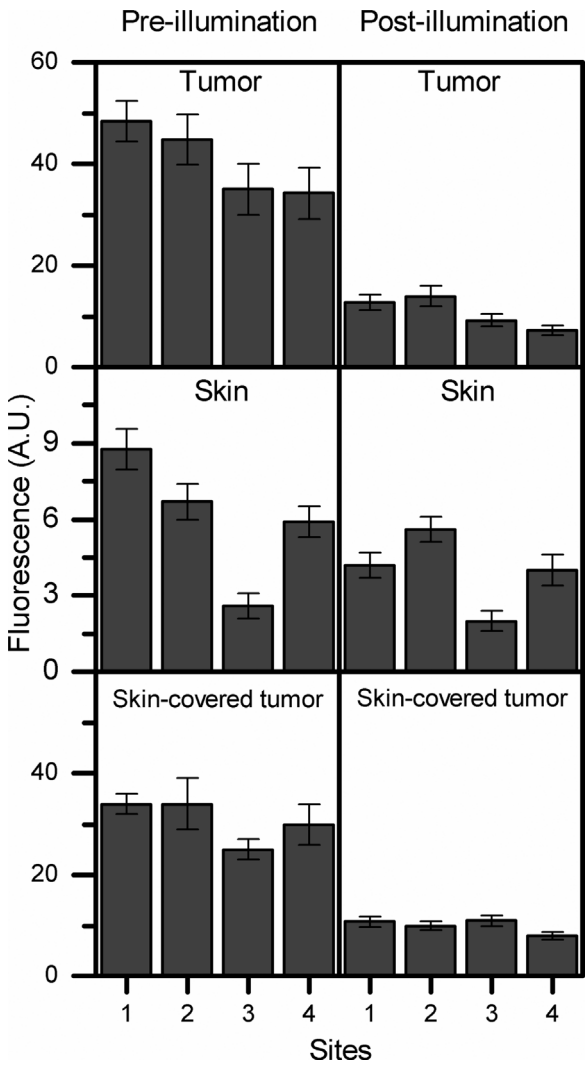


**Fig. 11.** Ex vivo fluorescence measurements from skin covered tumors, tumor without skin and skin separately, before and after illumination as indicated. In all the cases, the fiber optics was placed in the same spatial coordinates as depicted in Fig. 1.

fluorescence measurements from the skin-covered tumor, tumor and skin indicate that the skin contribution to the total fluorescence signal is about 15% and 30% before and after illumination, respectively. The contribution of the different planes of the tumor from the dermis to the peritoneal tissue is related to the dependence of the transmittance at 400 and 650 nm on the tumor thickness. Fluorescence measurements to infer the m-THPC concentration have been performed in different tumor models [22,56–59]. The pharmacokinetics of m-THPC in a rat fibrosarcoma tumor model indicates that the photosensitizer concentration in the tumor is about twice and 1.35 times the value obtained in the skin 48 and 72 h post-administration [58]. On the other hand, in a mesothelioma model the skin has larger drug absorption than the tumor [59]. For our tumor model, the florescence from the skin remains significantly smaller than from the tumor both at 48 and 72 h post-photosensitizer administration, as can be appreciated from data depicted in Figs. 4 and 11.

### 3.6. Evaluation of the PDT effect on tumors

The effect of the therapy was observed after 5 days of illumination; the tumor mass decreased and eschar formed in treated animals compared to control mice. The decrease in volume was not homogeneous, but more significant in the apical region, where the tumor was

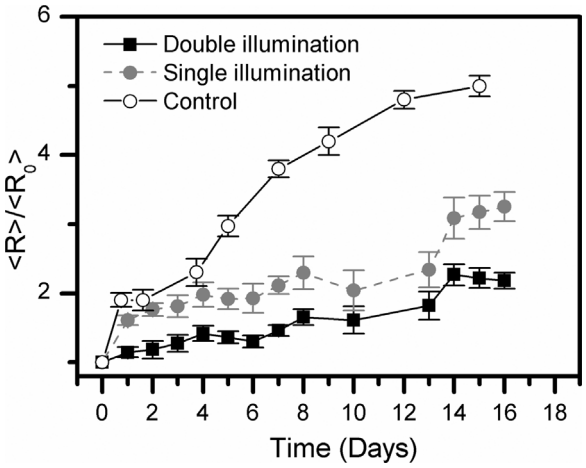


**Fig. 12.** Normalized tumor radio versus time of mice injected with m-THCP at a dose of 0.75 mg/kg and treated 24 and 48 h post-injection with single illumination (solid gray circles), with double illumination (solid squares) and control mice (open circles). Nine mice are considered and the standard errors are included.

illuminated directly, while caudal, cranial, ventral and dorsal zones received the light tangentially.

In the case of the highest dose tested, damage elsewhere in the mouse, including the tail, makes the procedure not advisable. In these cases, it is necessary to be extremely careful to avoid exposure of the mouse to sunlight. While data show that there is greater availability of drugs for the photochemical reaction, surrounding regions can be damaged, making the therapy less controllable. Furthermore, the photochemical reaction generates heat, making the therapy less tolerable.

The average tumor radius, measured as the average of the maximum and minimum tumor radii ($R$), divided by the initial tumor radius ($R_0$) was used to quantify the evolution of the tumor size (Fig. 12). The tumor growth rate decreased significantly in the case of treated mice in comparison with control ones. A second illumination after the “rebound effect” statistically improved the PDT treatment outcome as shown in Fig. 12, although for this type of tumor and for the experimental setup used to perform the illumination, a more significant improvement of the treatment cannot be expected. The main objective of the work was to show the importance of fluorescence measurements to follow the evolution of the photosensitizer concentration during the PDT treatment. Thanks to this, we were able to observe the “rebound effect” and employ it to guide a second illumination. It has recently been reported that light fractionation, consisting of two light dose applications 4 h apart, increases the efficacy of 5-aminolevulinic acid based PDT in normal mouse skin [60]. The “rebound effect” is locally relevant, as has been shown in this work by fluorescence measurements at different sites of the tumor. These results are associated with the tumor heterogeneity reflected in differences of photosensitizer level and oxygen concentration, as has been reported [61]. In fact, vascular damage plays a key role in determining the PDT outcome and depends on the basement membrane [38,61]. The imaging of the tumor vessels after PDT has been proposed as a valuable marker to predict the effectiveness of the treatment [62]. In any case, the average fluorescence measurements at different sites of the tumor, the “rebound effect”, can be detected and appear to be useful to guide a second illumination [41].

## 4. Conclusions

In this work, the in vivo follow-up of photosensitizer fluorescence in the tumor model to check the effectiveness of the PDT reaction is described.

After 24–96 h of the photosensitizer injection, the fluorescence signal reached a plateau (Figs. 3 and 4), and at any site of the tumor the intensity was larger than that obtained in the armpit of mice. Thus, the

preferential accumulation of the drug in the neoplastic tissue was tested. The dispersion of fluorescence values measured at different sites of the tumor is consistent with the large heterogeneity of these tumors.

The decrease in the fluorescence after the first illumination indicates the extent of the photochemical reaction, which was significantly smaller at the lateral sites than at the apical ones. In most cases, 24 h after the first illumination the intensity of the fluorescence signal increased again, showing the "rebound effect" depicted in Figs. 6 and 7 for different drug concentrations (0.75 mg/kg and 1.4 mg/kg) and absorption times (48, 72 and 96 h). The "rebound effect" was scarcely observed in laterals zones of the tumor; the decrease in the tumor volume was not homogeneous, but more evident in the apical region, where the tumor was illuminated perpendicularly.

Ex vivo fluorescence measurements performed at different sites in the skin covered tumor, the tumor without skin and the skin above the tumor, allows the evaluation of the contribution of both the tumor and the skin to the total fluorescence signal measured in vivo. The results indicate that the contribution from the tumor is significantly larger than that from the skin.

The results reveal the importance of using fluorescence to monitor the accumulation of the photosensitizer in the affected tissue. Furthermore, by monitoring the fluorescence after illumination, it is possible to take advantage of the "rebound effect" to improve the outcomes of PDT treatment.

The results are encouraging enough to continue to try to reach the interdisciplinary optimization of PDT work in the proposed model. The PDT can be presented as an advantageous alternative to palliative or curative cancer treatment and therefore may be sufficiently widespread. Fluorescence detection could also be better exploited not only to determine tumor location but also to enhance therapy.

## Acknowledgements

The authors thank Eng. Anibal Laquidara, Dr. Fausto Bredice, and Eng. Pablo Ixtaina for their electronic, spectrometric and photometric-radiometric contributions, respectively. MAP and MG are member of the research career at the Consejo Nacional de Investigaciones Científicas y Técnicas (CONICET). This work received financial support from (CONICET) (PIP 0602), Universidad Nacional de La Plata (UNLP) grants through Facultad de Ciencias Médicas (11-M/170) and Facultad de Ingeniería (11-I/170), and the Fundación Innovatec, Argentina (3/2014).

## References

[1] R.R. Allison, K. Moghissi, Oncologic photodynamic therapy: clinical strategies that modulate mechanisms of action, Photodiagnosis Photodyn. Ther. 10 (2013) 331–341.
[2] A.P. Castano, T.N. Demidova, M.R. Hamblin, Mechanism in photodynamic therapy: part one –photosensitizers, photochemistry and cellular locations, Photodiagnosis Photodyn. Ther. 1 (2004) 279–293.
[3] M.T. Jarvi, M.S. Patterson, B.C. Wilson, Insights into photodynamic therapy dosimetry: simultaneous singlet oxygen luminescence and photosensitizer photobleaching measurements, Biophys. J. 102 (2012) 661–671.
[4] F. Stewart, P. Baas, W. Star, What does photodynamic therapy have to offer radiation oncologists (or their cancer patients)? Radiother. Oncol. 48 (1998) 233–248.
[5] T.S. Mang, Lasers and light sources for PDT: past, present and future, Photodiagnosis Photodyn. Ther. 1 (2004) 43–48.
[6] T.J. Dougherty, D.G. Boyle, K.R. Weishaupt, Photoradiation therapy of human tumors, in: James D. Regan, John A. Parrish (Eds.), The Science of Photomedicine, Plenum Press, New York, 1982, pp. 625–638.
[7] T.J. Dougherty, J.E. Kaufman, A. Goldfarb, K.R. Weishaupt, D. Boyle, A. Mittleman, Photoradiation therapy for the treatment of malignant tumors, Cancer Res. 38 (1978) 2628–2635.
[8] T.J. Dougherty, G. Lawrence, J.H. Kaufman, D. Boyle, K.R. Weishaupt, A. Goldfarb, Photoradiation in the treatment of recurrent breast carcinoma, J. Natl. Cancer Inst. 62 (1979) 231–237.
[9] B.C. Wilson, M.S. Patterson, The physics, biophysics and technology of photodynamic therapy, Phys. Med. Biol. 53 (2008) R61–R109.
[10] A.P. Castano, T.N. Demidova, M.R. Hamblin, Mechanism in photodynamic therapy: part two –cellular signaling, cell metabolism and modes of cell death, Photodiagnosis Photodyn. Ther. 2 (2005) 1–23.
[11] A.P. Castano, T.N. Demidova, M.R. Hamblin, Mechanism in photodynamic therapy: part three –photosensitizer pharmacokinetics, biodistribution, tumor localization and mode of tumor destruction, Photodiagnosis Photodyn. Ther. 2 (2005) 91–106.
[12] R.R. Allison, G.H. Downie, R. Cuenca, X.-H. Hu, C.J.H. Childs, C.H. Sibata, Photosensitizers in clinical PDT, Photodiagnosis Photodyn. Ther. 1 (2004) 27–42.
[13] V.H. Fingar, T.J. Wieman, S.A. Wiehle, P.B. Cerrito, The role of microvascular damage in photodynamic therapy: the effect of treatment on vessel constriction, permeability, and leukocyte adhesion, Cancer Res. 52 (1992) 4914–4921.
[14] H.H. Buzzá, L.V. Silva, L.T. Moriyama, V.S. Bagnato, C. Kurachi, Evaluation of vascular effect of photodynamic therapy in chorioallantoic membrane using different photosensitizers, J. Photochem. Photobiol. B 138 (2014) 1–7.
[15] A.P. Castano, P. Mroz, M.R. Hamblin, Photodynamic therapy and anti-tumor immunity, Nat. Cancer Rev. 6 (2006) 535–545.
[16] Y. Zheng, G. Yin, V. Le, A. Zhang, S. Chen, X. Liang, J. Liu, Photodynamic-therapy activates immune response by disrupting immunity homeostasis of tumor cells, which generates vaccine for cancer therapy, Int. J. Biol. Sci. 12 (2016) 120–132.
[17] N. Maeding, T. Verwanger, B. Krammer, Boosting tumor-specific immunity using PDT, Cancers 8 (2016) 91, http://dx.doi.org/10.3390/cancers8100091.
[18] R.L. Lipson, E.J. Baldes, A.M. Olsen, The use of derivative of hematoporphyrin in tumor detection, J. Natl. Cancer Inst. 26 (1961) 1–11.
[19] K. Plaetzer, B. Krammer, J. Berlanda, F. Berr, T. Kiesslich, Photophysics and photochemistry of photodynamic therapy: fundamental aspects, Lasers Med. Sci. 24 (2009) 259–268.
[20] Photodynamic medicine. From bench to clinic, in: H. Koston, T. Hasan, L. Rhodes, E. Sage, M. Trotta (Eds.), Comprehensive Series in Photochemical and Photobiological Science, The Royal Society of Chemistry, 2016 (Cambridge, UK).
[21] J.P. Celli, B.Q. Spring, I. Rizvi, C.L. Evans, K.S. Samkoe, S. Verma, B.W. Pogue, T. Hasan, Imaging and photodynamic therapy mechanisms, monitoring, and optimization, Chem. Rev. 110 (2010) 2795–2838.
[22] L. Morlet, V. Vonarx-Coinsmann, P. Lenz, M.T. Foultier, L.X. de Brito, C. Stewart, T. Patrice, Correlation between meta(tetrahydroxyphenyl)chlorin (m-THPC) biodistribution and photodynamic effects in mice, J. Photochem. Photobiol. B: Biol. 28 (1995) 25–32.
[23] L. Morlet, V. Vonarx-Coinsmann, M.-T. Foultier, A. Gouyette, C. Stewart, P. Lenz, T. Patrice, In vitro and in vivo spectrofluorometry of water-soluble *meta*-(tetrahydroxyphenil) chlorin (m-THPC) derivative, J. Photochem. Photobiol. B: Biol. 39 (1997) 249–257.
[24] D.R. Braichotte, J.-F. Savary, P. Monnier, H.E. van den Bergh, Optimizing light dosimetry in photodynamic therapy of early stage carcinomas of the esophagus using fluorescence spectroscopy, Laser Surg. Med. 19 (1996) 340–346.
[25] M. Zellweger, P. Grosjean, P. Monnier, H. van den Bergh, G. Wagnières, Stability of the fluorescence measurement of foscans in the normal human oral cavity as an indicator of its content in early cancers of the esophagus and the bronchi, Photochem. Photobiol. 69 (1999) 605–610.
[26] W. Potter, T.S. Mang, T.J. Dougherty, The theory of photodynamic therapy dosimetry: consequences of photodestruction of sensitizer, Photochem. Photobiol. 46 (1987) 97–101.
[27] B. Liu, T.J. Farrell, M.S. Patterson, Comparison of noninvasive photodynamic therapy dosimetry methods using a dynamic model of ALA-PDT of human skin, Phys. Med. Biol. 57 (2012) 825–841.
[28] R.M. Valentine, C.T.A. Brown, H. Moseley, S. Ibbotson, K. Wood, Monte Carlo modeling of in vivo protoporphyrin IX fluorescence and singlet oxygen production during photodynamic therapy for patients presenting superficial basal cell carcinomas, J. Biomed. Opt. 16 (048002) (2011) 1–12.
[29] R. Cheung, M. Solonenko, T.M. Busch, F. Del Piero, M.E. Putt, S.M. Hahn, A.G. Yodh, Correlation of *in vivo* photosensitizer fluorescence and photodynamic-therapy-induced depth of necrosis in a murine tumor model, J. Biomed. Opt. 8 (2003) 248–252.
[30] J. Barge, T. Glanzmann, M. Zellweger, D. Salomon, H. van den Bergh, G. Wagnières, Correlations between photoactivable porphyrins fluorescence, erythema and the pain induced by PDT on normal skin using ALA-derivatives, Photodiagnosis Photodyn. Ther. 10 (2013) 683–693.
[31] A. Johansson, F. Faber, G. Knieböhler, H. Stepp, R. Sroka, R. Egensperger, W. Beyer, F.W. Kreth, Protoporphyrin IX fluorescence and photobleaching during interstitial photodynamic therapy of malignant gliomas for early treatment prognosis, Lasers Surg. Med. 45 (2013) 225–234.
[32] J.C. Finlay, S. Mitra, T.H. Foster, Foster In vivo mTHPC photobleaching in normal rat skin exhibits unique irradiance-dependent features, Photochem. Photobiol. 75 (2002) 282–288.
[33] J.C. Finlay, S. Mitra, M.S. Patterson, T.H. Foster, Photobleaching kinetics of photofrin in vivo and in multicell tumor spheroids indicate two simultaneous bleaching mechanisms, Phys. Med. Biol. 49 (2004) 4937–4960.
[34] J.S. Dysart, G. Singh, M.S. Patterson, Calculation of singlet oxygen dose from photosensitizer fluorescence and photobleaching during m-THC photodynamic therapy of MLL cells, Photochem. Photobiol. 81 (2005) 196–205.
[35] F. Zhou, W.R. Da Xing, Chen Dynamics and mechanism of HSP70 translocation induced by photodynamic therapy treatment, Cancer Lett. 264 (2008) 135–144.
[36] A. Chiaviello, I. Postiglione, G. Palumbo, Targets and mechanisms of photodynamic therapy in lung cancer cells: a brief overview, Cancers 3 (2011) 1014–1041.
[37] T. Windahl, Q. Peng, J. Moan, S. Hellsten, B. Axelsson, L. Löfgren, Uptake and distribution of intravenously or intravesically administered photosensitizers in the rat, Cancer Lett. 75 (1993) 65–70.
[38] J.C. Finlay, D.L. Conover, E.L. Hull, T.H. Foster, Porphyrin bleaching and PDT-induced spectral changes are irradiance dependent in ALA-sensitized normal rat skin in vivo, Photochem. Photobiol. 73 (2001) 54–63.

[39] B. Kruijt, A. van der Ploeg-van den Heuvel, H.S. de Bruijn, H.J.C.M. Sterenborg, A. Amelink, D.J. Robinson, Monitoring interstitial m-THPC-PDT in vivo using fluorescence and reflectance spectroscopy, Laser Surg. Med. 41 (2009) 653–664.
[40] K.R. Rollakanti, S.C. Kanick, S.C. Davis, B.W. Pogue, E.V. Maytin, Techniques for fluorescence detection of protoporphyrin IX in skin cancers associated with photodynamic therapy, Photonics Lasers Med. 2 (2013) 287–303.
[41] B.W. Pogue, J.T. Elliott, S.L. Kanick, S.C. Davis, K.S. Samkoe, E.V. Maytin, S.P. Pereira, T. Hasan, Revisiting photodynamic therapy dosimetry: reductionist and surrogate approaches to facilitate clinical success, Phys. Med. Biol. 61 (2016) R57–R89.
[42] M.L. Kripke, E. Gruys, I.J. Fidler, Metastatic heterogeneity of cells from an ultraviolet light-induced murine fibrosarcoma of recent origin, Cancer Res. 38 (1978) 2962–2967.
[43] R. Kearney, A. Basten, D.S. Nelson, Cellular basis for the immune response to methylcholanthrene-induced tumors in mice. Heterogeneity of effector cells, Int. J. Cancer 15 (1975) 438–450.
[44] C.P. Sabino, A.M. Deanna, T.M. Yoshimura, D.F.T. da Silva, C.M. França, M.R. Hamblin, M.S. Ribeiro, The optical properties of mouse skin in the visible and near infrared spectral regions, J. Photochem. Photobiol. B: Biol. 160 (2016) 72–78.
[45] J.R. Lakowicz, Principles of Fluorescence Spectroscopy, third ed., Springer Publisher, NewYork, 2006.
[46] M.O. Senge, J.C. Brandt, Temoporfin (Foscan®, 5,10,15,20-tetra(m-hydroxyphenyl) chlorin)–a second-generation photosensitizer, Photochem. Photobiol. 87 (2011) 1240–1296.
[47] M.E. Etcheverry, M.A. Pasquale, M. Garavaglia, Photodynamic therapy of HeLa cell cultures by using LED or laser sources, J. Photochem. Photobiol. B: Biol. 160 (2016) 271–277.
[48] S. Anbil, I. Rizvi, J.P. Celli, N. Alagic, T. Hasan, A photobleaching-based PDT dose metric predicts PDT efficacy over certain BPD concentration ranges in a three-dimensional model of ovarian cancer, Progress in Biomedical Optics and Imaging-Proceeding of SPIE (2017) 8568 (201117/12.2010840).
[49] I. Rizvi, S. Anbil, N. Alagic, J.P. Celli, L.Z. Zheng, A. Palanisami, M.D. Glidden, B.W. Pogue, T. Hasan, PDT dose parameters impact tumoricidal durability and cell death pathways in a 3D ovarian cancer model, Photochem. Photobiol. 89 (2013) 942–952.
[50] A.L. Maas, S.L. Carter, E.P. Wileyto, J. Miller, M. Yuan, G. Yu, A.C. Durham, T.M. Busch, Tumor vascular microenvironment determines responsiveness to photodynamic therapy, Cancer Res. 72 (2012) 2079–2088.
[51] C. Michiels, C. Tellier, O. Feron, Cycling hypoxia: a key feature of the tumor microenvironment, Biochim. Biophys. Acta (BBA) –Rev. Oncancer 1866 (2016) 76–86.
[52] J.A. Ju, I. Godet, I.C. Ye, J. Byun, H. Jayatilaka, S.J. Lee, L. Xiang, D. Samanta, M.H. Lee, P.-H. Wu, D. Wirtz, G.L. Semenza, D.M. Gilkes, Hypoxia selectively enhances integrin α5β1 receptor expression in breast cancer to promote metastasis, Mol. Cancer Res. 15 (2017) 1–12 (0.1158/1541-7786).
[53] C. Sheng, B.W. Pogue, H. Dehghani, S.A. ÓHara, P.J. Hoopes, Numerical light dosimetry in murine tissue analysis of tumor curvature and angle incidence effects upon fluence in the tissue. In Optical methods for tumor treatment and detection. Mechanisms and techniques in photodynamic therapy VII, in: D. Kessel (Ed.), Proc. of SPIE, 4952 2003, pp. 39–47.
[54] P. Cramers, M. Ruevekamp, H. Oppelaar, O. Dalesio, P. Baas, F.A. Stewart, Foscan® uptake and tissue distribution in relation to photodynamic efficacy, Br. J. Cancer 88 (2003) 283–290.
[55] C.P. Sabino, A.M. Deana, D.F.T. Silva, C.M. França, T.M. Yoshimura, M.S. Ribeiro, Optical properties of mice skin for optical therapy relevant wavelengths: influence of gender and pigmentation, Proc. of SPIE Mechanisms for Low-Light Therapy X (2015) 93090D 93090D. 10.1117/12.2080853; https://doi.org/10.1117/12.2080853.
[56] J. Johansson, R. Berg, K. Svanberg, S. Svanberg, Laser-induced fluorescence studies of normal and malignant tumor tissue of rat following intravenous injection of δ–amino levulinic acid, Laser Surg. Med. 20 (1997) 272–274.
[57] W. Alian, S. Andersson-Engels, K. Svanberg, S. Svanberg, Laser-induced fluorescence studies of meso-tetra(hydroxyphenyl)chlorin in malignant and normal tissues in rats, Br. J. Cancer 70 (1994) 980–885.
[58] H.J. Jones, D.I. Vernon, S.B. Brown, Photodynamic therapy effect of m-THPC (Foscan®) in vivo: correlation with pharmacokinetics, Brit. J. Cancer 89 (2003) 398–404.
[59] P. Cramers, M. Ruevekamp, H. Oppelaar, O. Dalesio, P. Baas, F.A. Stewart, Foscan® uptake and tissue distribution in relation to photodynamic efficacy, Brit. J. Cancer 88 (2003) 283–290.
[60] H.S. de Bruijn, S. Brooks, A. van der Ploeg-van den Heuvel, T.L.M. ten Hagen, E.R.M. de Haas, D.J. Robinson, Light fractionation significantly increases the efficacy of photodynamic therapy using BF-200 ALA in normal mouse skin, PLoS One 11 (2017) e0148850, http://dx.doi.org/10.1371/journal.pone.0148850.
[61] S.M. Hahn, M.E. Putt, J. Metz, D.B. Shin, E. Rickter, C. Menon, D. Smith, E. Glatstein, D.L. Fraker, T.M. Busch, Photofrin uptake in tumor and normal tissues of patients receiving intraperitoneal photodynamic therapy, Clin. Cancer Res. 12 (2006) 5464–5470.
[62] T.J.L. Schreurs, S.J. Hectors, I. Jacobs, H. Grull, K. Nicolay, G.J. Strijkers, Quantitative multi-parametric magnetic resonance imaging of tumor response to photodynamic therapy, PLoS One 11 (11) (2016) e0165759, http://dx.doi.org/10.1371/jounal.pone.016579.